

Removal of nitrogen from simulated ground water by scoria: dynamic processes and modeling

Tianzi Dong^{a,b,c}, Yuling Zhang^{a,b,c,*}, Xiaosi Su^{b,c}, Rui Li^{a,b,c}

^aCollege of Environment and Resources, Jilin University, Changchun 130021, China

^bKey Laboratory of Groundwater Resources and Environment, Ministry of Education, Jilin University, Changchun 130021, China

^cInstitute of Water Resources and Environment, Jilin University, Changchun 130021, China, Tel. +8613756160831, email: lingling29@126.com (Y. Zhang)

Received 27 March 2017; Accepted 23 July 2017

ABSTRACT

In this study, the dynamic processes of nitrogen removal from aqueous solutions were identified. The study used column experiments at different influent flow rates (40 mL/min, 60 mL/min and 80 mL/min) and different nitrogen concentrations (1 mg/L, 2 mg/L, and 5 mg/L for $\text{NH}_4^+\text{-N}$ and $\text{NO}_2^-\text{-N}$; 30 mg/L, 50 mg/L, and 80 mg/L for $\text{NO}_3^-\text{-N}$). The adsorption data for nitrogen fitted well with the Thomas and Yoon-Nelson models. At different filled heights (0.5 m, 0.75 m, and 1.0 m), the adsorption data fitted well with the Bed Depth Service Time model. The back-flush method can enable scoria to recover purification efficiency. After seven back flushes, the regeneration rate was better than 90%. Breakthrough curves from tank experiments yielded very similar results to the column experiments. The breakthrough time of $\text{NH}_4^+\text{-N}$ and $\text{NO}_2^-\text{-N}$ in the tank experiments were almost the same as in the column experiments. However, the breakthrough time of $\text{NO}_3^-\text{-N}$ was slightly shorter than in column experiments.

Keywords: Scoria; Nitrogen adsorption; Dynamic processes; Modeling; Back flush

1. Introduction

With the rapid development of modern society, water shortages have become more prevalent. Water shortages caused by pollution are common. Millions of people worldwide are suffering from a shortage of potable drinking water [1]. In recent years, the discharge of industrial wastewater and the widespread use of agricultural fertilizer has led to excessive nitrogen in groundwater. This creates new challenges for the environment. Excessive nitrogen ingestion through drinking water is harmful to the human body. Blue-baby syndrome (methemoglobinemia) is related to nitrate ingestion. Nitrosamines are carcinogenic compounds that may be formed from nitrite in the stomach and lead to tumor growth and cancer [2]. According to China's "Hygienic standard for drinking water (GB5749-2006)",

ammonia nitrogen, nitrate, and nitrite in drinking water must not exceed 0.5, 20, and 1 mg/L, respectively.

Several methods have been identified for reducing nitrogen in water. The biological method [3], ion exchange [4], and adsorption denitrification [5] have been applied for the removal of excess ammonia nitrogen. Recently, as a result of low prices and effectiveness, the adsorption method has been widely used. Zeolite [6], clinoptilolite [7], and activated carbon [8] are the most widely used adsorbents for ammonium nitrogen removal. Jun-Boum performed tests on clinoptilolite to determine the factors controlling permeable reactive barriers to contaminated groundwater. The removal of ammonium and heavy metals was shown to be efficient in laboratory-scale experiments [9]. Clinoptilolite was used to remove ammonium from municipal landfill leachate. Fluidized-bed column experiments were studied to simulate the actual conditions. The effects of flow rate, ammonium concentration, and bed expansion in the column were analyzed. In addition, breakthrough modeling was applied [10]. Rice husk biochar was used to remove ammonium nitrogen

*Corresponding author.

from piggery manure anaerobic digestate slurry. Experiments were conducted using a fixed bed to investigate the effects of concentration, flow rate, and bed depth on ammonium adsorption. The breakthrough was then analyzed. Experimental data and commonly used models were fitted [11]. For the removal of nitrate nitrogen in water, biological [12], ion exchange [13] and adsorption methods [14] have been widely used. Activated carbon and other synthetic adsorbent are often used in adsorption technology. Wang conducted experiments using oak sawdust modified by lanthanum (La)-involved pyrolysis on the adsorption of ammonium, nitrate, and phosphate [15]. A synthesized polymeric adsorbent, modified by amino and quaternary ammonium groups, was shown to be effective for nitrate removal [16]. However, nitrite removal using the adsorption method has rarely been reported. In addition, the adsorption of ammonia nitrogen, nitrate nitrogen, and nitrite nitrogen by the same material has received little attention.

For these reasons, the present study investigated the effectiveness of scoria in removing nitrogen from groundwater. Scoria adsorbent is a natural material that can be easily exploited and has a reasonable price. It can be used to purify water in laboratory-scale experiments and also in actual water purification facilities. Scoria has been studied as an adsorbent of Cu^{2+} and Zn^{2+} in water [17,18]. In addition, experiments have also been conducted on the removal of petroleum hydrocarbons [19] and fluoride [20] from groundwater. The present study represents the first attempt to investigate adsorption by scoria in the removal of nitrogen from groundwater using a column and tank reactor. In the column reactor experiments, factors which affect flow rate (inlet concentration and filler height) were analyzed. Generally used models were applied to describe the breakthrough. Then column regeneration was examined using back flushing. Finally, seepage tank reactor experiments were conducted and nitrogen change rules for the effluent were obtained.

The column and tank reactor dynamic experiment conditions were set according to the characteristics of a real-world study area. The study area is located in northeastern China, alongside a river. The hydrogeological conditions are as follows: the main aquifer is unconfined and comprises Quaternary unconsolidated sands, gravels, and underlying Cretaceous mud shale. The aquifer thickness is 18–25 m and groundwater depth is 2–5 m. The aquifer thickness varies slightly. The water quality conditions are as follows: the hydrochemical type is HCO_3^- -Ca, pH ranges from 6 to 8. The NH_4^+ -N concentration is 0.29–3.67 mg/L. NH_4^+ -N that exceeds the limits imposed by China's drinking water standards is mainly concentrated in the 1.0–3.0 mg/L range. Iron and manganese levels generally exceed China's water standard limits. The Fe^{2+} concentration is 0.1–18.0 mg/L and Mn^{2+} is 0.1–10 mg/L. Other water chemical compositions tested do not exceed China's "Hygienic standard for drinking water (GB5749-2006)".

2. Materials and methods

2.1. Materials

Scoria is a natural, commercially available, product. It was purchased in northeast China, where rich scoria

resources exist. After sieving, the particle size was mainly distributed in the 0.25 mm to 2.0 mm range. The purchase price was approximately 100 RMB/m³. Thus, it is easily affordable for use as a purifier. Scoria is mainly made up of pores, minerals, and volcanic glass. It is mainly composed of quartz, alkali feldspar, and plagioclase. It is gray and black in color. Its BET specific surface is high (30–150 m²/g) as is its porosity (74%–78%). These characteristics can enhance the removal of NH_4^+ -N, NO_2^- -N, and NO_3^- -N from water. In addition, scoria is lightweight as a result of its loose bulk density (500–600 kg/m³). Thus, scoria has application potential in water purification technologies.

2.2. Methods

2.2.1. Dynamic seepage column reactor experiments

The influent pattern was down-flow. Scoria was evenly filled in the seepage columns without air bubbles, and quartz sand was selected as the supporting layer for 2–3 mm to provide a uniform inlet flow. The actual drinking water demand of Chinese rural residents was used as the basis for the seepage column flow rates and was set at 40 mL/min–80 mL/min. The initial nitrogen solution concentrations were set according to actual nitrogen concentrations in the study area. The nitrogen solution was prepared by dissolving analytical-grade NH_4Cl , NaNO_2 , and NaNO_3 . Initially, experiments were conducted in a glass column with a 4.00 cm diameter and a 0.5 m height. The initial flow rate was set to 60 mL/min, and the influent concentration (mg/L) of NH_4^+ -N, NO_2^- -N, and NO_3^- -N was 1, 1, and 30, respectively. Then the seepage column height was increased to 0.75 m, while the flow rate and influent concentration were the same as above. Finally the seepage height was increased to 1.0 m. Flow rates (mL/min) of 40, 60, and 80 were applied. For these flow rates the influent concentrations (mg/L) were: 1, 2, and 5, respectively, for NH_4^+ -N; 1, 2, and 5, respectively, for NO_2^- -N; and 30, 50, and 80, respectively, for NO_3^- -N. Samples were taken and tested at specific times from the bottom of the seepage column until breakthrough occurred. The test method is referred to as the "water and wastewater monitoring analysis method (the 4th Edition)". Schematic of seepage column reactor is shown in Fig. 1.

After the exhaustion of the columns, back-flush experiments were conducted to recover the breakthrough col-

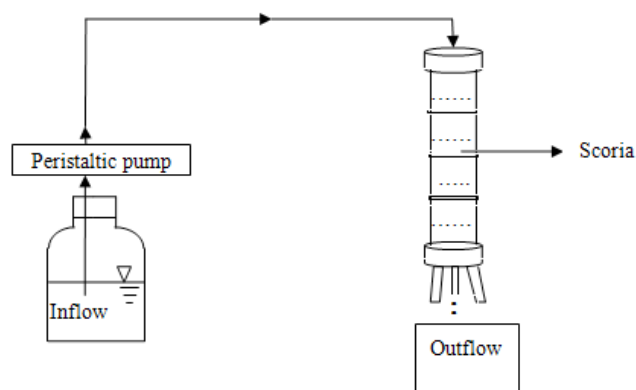


Fig. 1. Schematic of seepage column reactor.

umns. The back-flush flow rate was determined when the scoria was slightly disturbed by the back-flush water. The back-flush time was recorded from the start to the end of the time needed to clean the material. The purification efficiency after back flushes was analyzed.

2.2.2. Dynamic seepage tank reactor experiments

The main body of the seepage tank was composed of 0.6 cm thick organic glass. The ends were separated 5 cm into the inlet sink and outlet sink with porous filter plates. The active part of the seepage tank was 20 cm long, 15 cm wide, and 20 cm high. The influent pattern was horizontal flow through a side wall of the tank. The flow rate was 60 mL/min. The influent concentration (mg/L) of $\text{NH}_4^+\text{-N}$, $\text{NO}_2^-\text{-N}$, and $\text{NO}_3^-\text{-N}$ was 2, 2, and 30, respectively. Samples were taken at specific times at the inlet until breakthrough. Schematic of seepage tank reactor is shown in Fig. 2.

3. Results and discussion

3.1. Seepage column reactor adsorption performance

3.1.1. Effect of flow rate

Flow rate is an important factor that can greatly affect the performance of adsorbent. The effect of flow rate on the adsorption was investigated by columns with a diameter of 4 cm and depth of 1 m. The flow rate (mL/min) was set at 40, 60, and 80, and the influent concentration (mg/L) of $\text{NH}_4^+\text{-N}$, $\text{NO}_2^-\text{-N}$, and $\text{NO}_3^-\text{-N}$ was 1, 1, and 30, respectively. Breakthrough curves for the adsorption of $\text{NH}_4^+\text{-N}$, $\text{NO}_2^-\text{-N}$, and $\text{NO}_3^-\text{-N}$ onto scoria at different flow rates are presented in Fig. 3. The latest breakthrough and exhaustion was observed at the lowest flow rate (40 mL/min). At higher flow rates (60 and 80 mL/min) the breakpoint moved to the left and breakthrough curves became steeper. Consequently, the breakpoint time became shorter. A plausible explanation might be that with the smaller flow rate, the breakthrough time in the columns is longer and adsorption occurred more completely. When the flow rate is faster, the contact time between nitrogen and scoria is short. This limits the combination of nitrogen with available adsorption sites and the intra-particle diffusion into the pores of scoria. Karadag et al. studied NH_4^+ adsorption onto clinoptilolite-fixed bed columns using municipal landfill leachate, and found that the increase in flow rates led to total removal efficiency at the exhaustion point. It was suggested that the lower removal efficiency and capacity values were a result of the insufficient retention time for the complete exchange

of ammonium ions in the clinoptilolite bed [10]. Wu et al. modified a polymeric adsorbent with amino and quaternary ammonium groups for the purpose of nitrate removal from water. They observed the effect of the flow rate. The breakthrough point appeared at a smaller bed volume and the breakthrough curves reached the saturated point faster as the flow rate increased [16].

3.1.2. Effect of initial influent concentration

Initial influent concentration is also significant because of its influence on the dynamic performance of the adsorbent. The effect of initial concentrations on the adsorption of $\text{NH}_4^+\text{-N}$, $\text{NO}_2^-\text{-N}$, and $\text{NO}_3^-\text{-N}$ was investigated by columns with a 4 cm diameter and a 1 m depth. The flow rate (mL/min) was set at 60. The initial influent concentrations (mg/L) for $\text{NH}_4^+\text{-N}$ were 1, 2, and 5. The same initial values were used for $\text{NO}_2^-\text{-N}$ concentrations. The initial influent concentrations (mg/L) for $\text{NO}_3^-\text{-N}$ were 30, 50, and 80. Breakthrough curves are shown in Fig. 4. An obvious trend was observed when a high concentration nitrogen solution was used; the breakpoint moved to the left and the breakthrough curves became steeper, leading to a reduced exhaustion time for the seepage columns. The results obtained illustrate that the concentration gradient is one of the most significant effects of the adsorption saturation, and thus acts as a driving force for the adsorption process. At high influent concentration, more scoria adsorption sites are increasingly surrounded to accommodate nitrogen. Consequently, the driving force increases, the adsorption rate accelerates, the migration and diffusion coefficient becomes large, and the time for adsorption sites on the surface of the scoria to reach saturation is short. Thus, the time required for breaking the seepage column is short. Similar results were concluded by other researchers. Mashal et al. removed ammonia from aqueous solutions using a natural zeolite fixed-bed. When a high initial concentration of ammonia was used, the breakthrough curves were sharp and steep, indicating fast exhaustion of the bed. The time needed to reach the breakpoint increased as the initial ammonia concentration in the solution was decreased [21]. Zhu modified porous zeolite pellets to remove ammonia nitrogen from water. In terms of reaching the breakthrough point, the lower the ammonia concentration, the better the treatment effect [22].

3.1.3. Effect of filled height

The experiments were conducted using seepage columns with a 4 cm diameter. The fill heights (m) were 0.5,

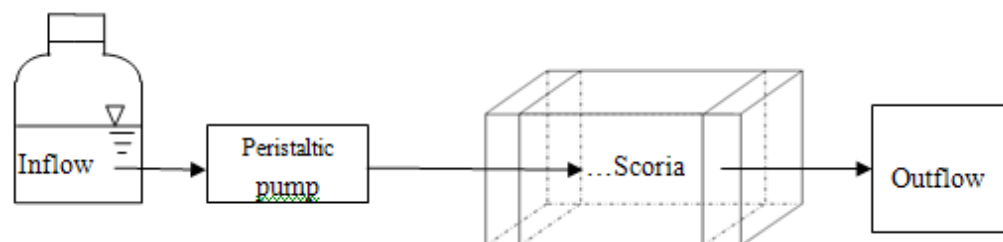
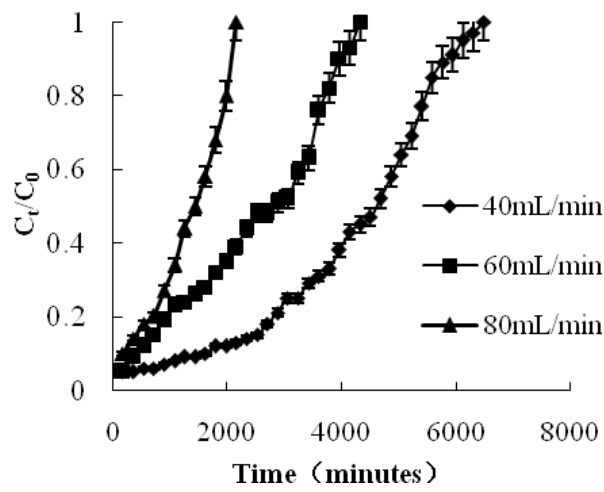
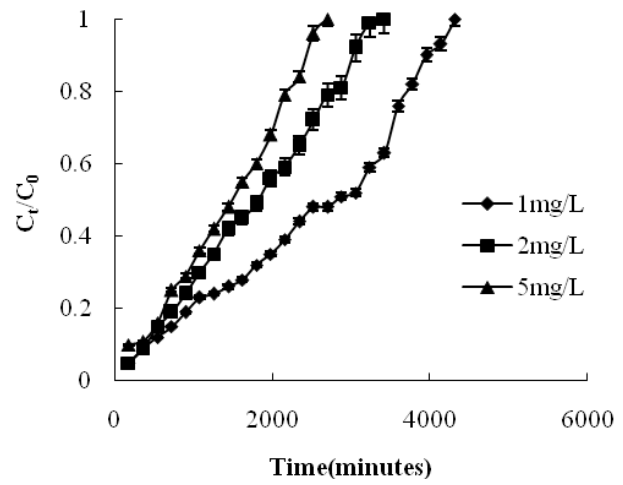


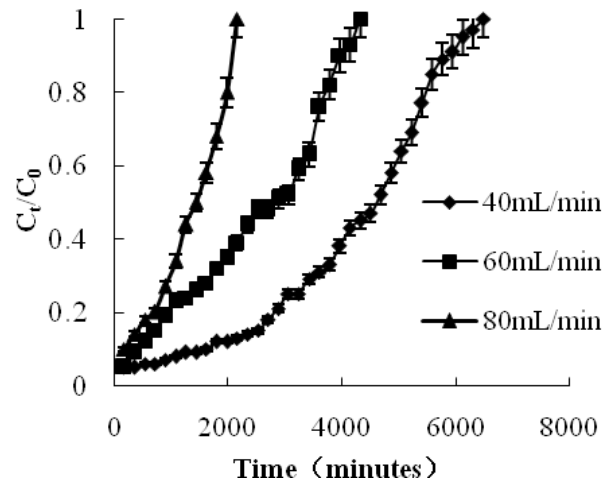
Fig. 2. Schematic of seepage tank reactor.



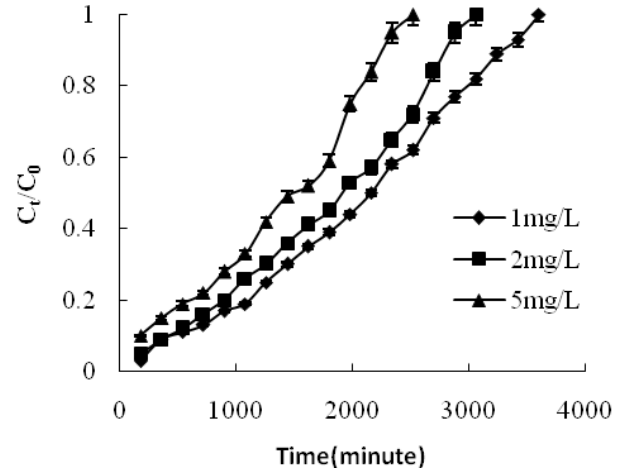
(a) $\text{NH}_4^+\text{-N}$



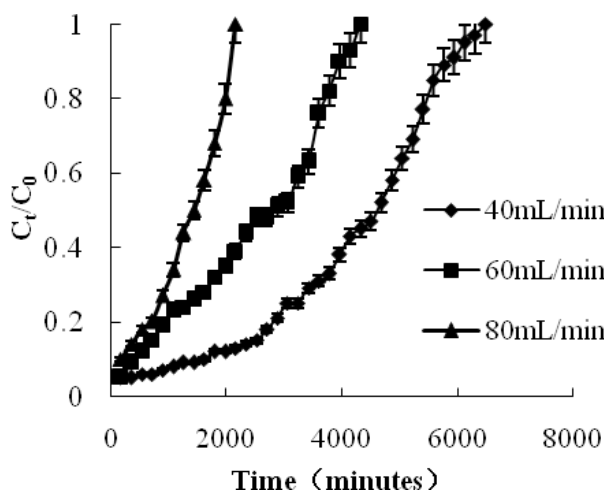
(a) $\text{NH}_4^+\text{-N}$



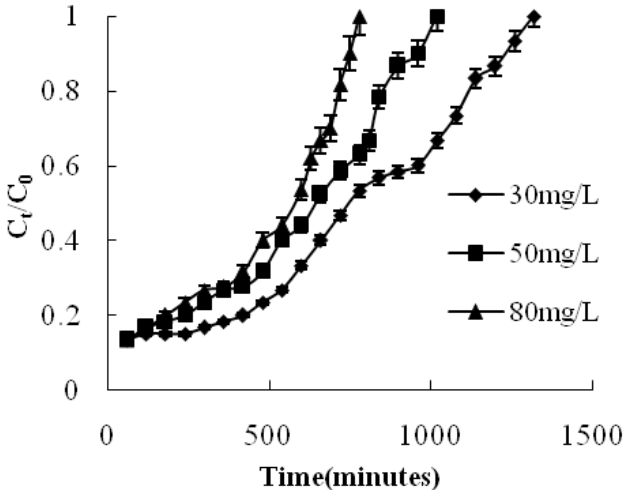
(b) $\text{NO}_2^-\text{-N}$



(b) $\text{NO}_2^-\text{-N}$



(c) $\text{NO}_3^-\text{-N}$



(c) $\text{NO}_3^-\text{-N}$

Fig. 3. Breakthrough curves for varying flow rates of $\text{NH}_4^+\text{-N}$, $\text{NO}_2^-\text{-N}$, and $\text{NO}_3^-\text{-N}$.

Fig. 4. Breakthrough curves for different initial concentrations of $\text{NH}_4^+\text{-N}$, $\text{NO}_2^-\text{-N}$, and $\text{NO}_3^-\text{-N}$.

0.75, and 1.0 m. The flow rate was set at 60 mL/min. The influent concentrations (mg/L) of $\text{NH}_4^+\text{-N}$, $\text{NO}_2^-\text{-N}$, and $\text{NO}_3^-\text{-N}$ were 1, 1, and 30. Breakthrough curves for adsorption at different fill heights are shown in Fig. 5. As the filled height was increased, the contact time between nitrogen and available scoria adsorption binding sites increased. Thus, for effluent solutions at the same elapsed time, the nitrogen concentration was lower with the increased fill height. In addition, when the fill height was increased, the breakthrough curve had a slower change trend. Consequently, the slope of the breakthrough curve decreased, indicating that the curve becomes steeper as the column fill height is decreased. The sorption process in the column was strongly influenced by the bed height. Similar results were concluded and the breakthrough point appeared at a larger bed volume when the resin bed was higher [16]. Mashal et al. removed ammonia from aqueous solutions using a natural zeolite fixed-bed. The time needed for the fixed-bed of zeolites to reach the saturation concentration increased with bed depth, which is proportional to the amount of zeolite in the column [21].

3.2. Modeling fixing

To analyze the dynamic process of adsorption onto an adsorbent, mathematical models are commonly used for fixing dynamic data. The Thomas, Yoon-Nelson, and Bed Depth Service Time (BDST) models are commonly used.

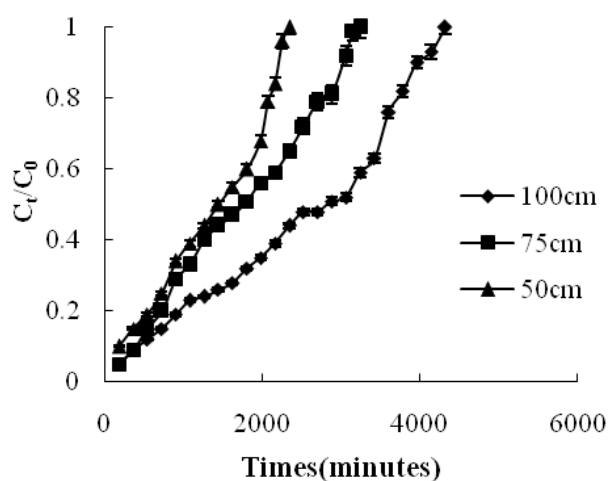
3.2.1. Thomas model

The Thomas model was proposed by Thomas [23] to analyze the breakthrough curves obtained from chromatography columns. In recent times, this model has been employed to fit experimental data and describe the dynamic adsorption curve. The linearized form is expressed as:

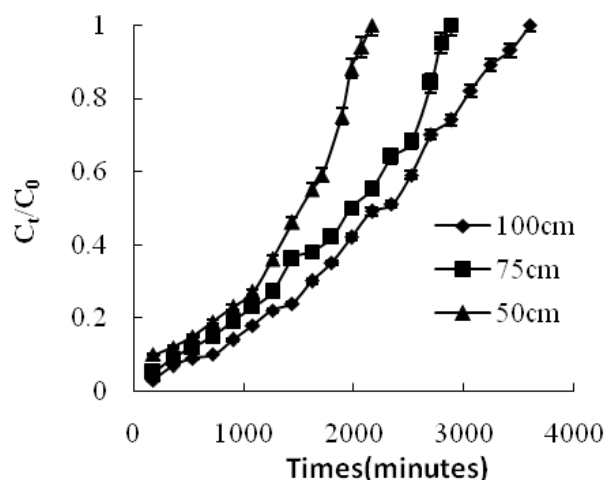
$$\ln\left(\frac{C_0}{C_t} - 1\right) = \frac{K_{TH}q_0M}{Q} - K_{TH}C_0t \quad (1)$$

where C_0 and C_t (mg/L) are influent and effluent concentrations, V (L) is the effluent volume, K_{TH} (L/mg/min) is the Thomas rate constant, q_0 (mg/g) is the adsorption capacity, Q is the flow rate, and M (g) is the weight of the scoria. The Thomas model is based on the assumption that adsorption is well-described by Langmuir kinetics and second-order reversible reaction kinetics [24]. The scoria adsorbent complies with the above two types of kinetics.

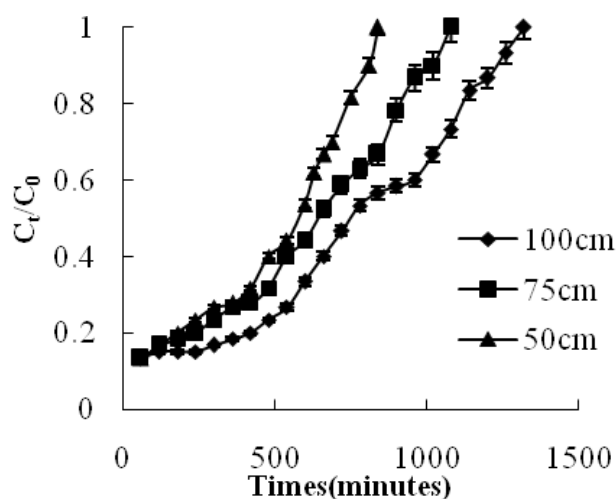
Parameters obtained using the Thomas model (varied flow rates and varied initial concentrations for $\text{NH}_4^+\text{-N}$, $\text{NO}_2^-\text{-N}$, and $\text{NO}_3^-\text{-N}$) are expressed in Tables 1 and 2. For the different flow rates, the correlation coefficients with the Thomas model were all better than 0.93. Therefore, the dynamic adsorption process of $\text{NH}_4^+\text{-N}$, $\text{NO}_2^-\text{-N}$, and $\text{NO}_3^-\text{-N}$ fitted well with the Thomas model. As shown in Table 1, K_{TH} increased as the inlet flow rate increased. In contrast, q_0 decreased as the inlet flow rate increased. This indicates that when the low rate increases, the resistance in the adsorption process decreases. Thus, the nitrogen solution in the columns had less hydraulic retention time and seepage columns could be more easily penetrated.



(a) $\text{NH}_4^+\text{-N}$



(b) $\text{NO}_2^-\text{-N}$



(c) $\text{NO}_3^-\text{-N}$

Fig. 5. Breakthrough curves for different filled heights of $\text{NH}_4^+\text{-N}$, $\text{NO}_2^-\text{-N}$, and $\text{NO}_3^-\text{-N}$.

Table 1
Parameters estimated by the Thomas model for different flow rates

Item	Flow rate (mL/min)	q_0 (mg/g)	K_{TH} (L/mg/min)	R^2
NH ₄ ⁺ -N	40	10.19	0.0009	0.931
	60	9.16	0.0011	0.941
	80	6.78	0.0019	0.988
NO ₂ ⁻ -N	40	7.44	0.0012	0.978
	60	7.20	0.0015	0.988
	80	5.12	0.0029	0.967
NO ₃ ⁻ -N	40	79.69	7.6×10 ⁻⁵	0.934
	60	77.61	1.1×10 ⁻⁴	0.946
	80	60.61	1.8×10 ⁻⁴	0.938

Table 2
Parameters estimated by the Thomas model for different initial concentrations

Item	Initial concentration (mg/L)	q_0 (mg/g)	K_{TH} (L/mg/min)	R^2
NH ₄ ⁺ -N	1	9.16	0.0011	0.941
	2	12.64	0.00085	0.901
	5	26.96	0.0004	0.943
NO ₂ ⁻ -N	1	7.20	0.0015	0.988
	2	13.56	0.00085	0.940
	5	25.29	0.00046	0.941
NO ₃ ⁻ -N	30	77.61	1.1×10 ⁻⁴	0.946
	50	89.99	7.0×10 ⁻⁵	0.957
	80	91.38	6.13×10 ⁻⁵	0.955

Regarding different initial concentrations, the correlation coefficients for the Thomas model were all better than 0.90, indicating a good fit between the experiment data and the Thomas model. As shown in Table 2, when the initial concentration was increased, K_{TH} decreased, whereas q_0 showed an increasing trend. With the increase in the initial nitrogen concentration, the adsorption rate was reduced. However, the increase in the concentration gradient led to an increased mass transfer driving force, which overcame the steric hindrance. Therefore, the number of active adsorption sites increases and adsorption quantity increases. Our results corroborate earlier findings. For example, Wang et al. developed a functionalized zeolite column to remove ammonia nitrogen from aqueous solution. The dynamic adsorption could be fitted by the Thomas model [25]. Xie et al. studied the dynamic adsorption of ammonia nitrogen by walnut shells, and found that the Thomas model reflects the characteristics of the adsorption process well [26].

3.2.2. Yoon-Nelson model

The Yoon-Nelson model was proposed by Yoon and Nelson [27] to analyze the breakthrough curves and adsorption of gases by activated biochar. In recent times, this model

Table 3
Parameters estimated by the Yoon-Nelson model for different flow rates

Item	Flow rate (mL/min)	τ (min)	K_{YN} (min ⁻¹)	R^2
NH ₄ ⁺ -N	40	4415	0.0009	0.931
	60	2480	0.0011	0.941
	80	1372	0.0019	0.988
NO ₂ ⁻ -N	40	2958	0.0012	0.978
	60	2000	0.0015	0.988
	80	1044	0.0029	0.967
NO ₃ ⁻ -N	40	1043	0.0023	0.934
	60	714	0.0035	0.946
	80	407	0.0054	0.938

Table 4
Parameters estimated by the Yoon-Nelson model for different initial concentrations

Item	Initial concentration (mg/L)	τ (min)	K_{YN} (min ⁻¹)	R^2
NH ₄ ⁺ -N	1	2480	0.0011	0.941
	2	1700	0.0017	0.901
	5	1450	0.002	0.943
NO ₂ ⁻ -N	1	2000	0.0015	0.988
	2	1823	0.0017	0.940
	5	1522	0.0023	0.941
NO ₃ ⁻ -N	30	714	0.0035	0.946
	50	542	0.0045	0.957
	80	500	0.005	0.955

has been widely used to describe the dynamic adsorption process. The linearized form of the model is expressed as:

$$\ln\left(\frac{C_0}{C_0 - C_t}\right) = K_{YN}t - \tau K_{YN} \quad (2)$$

where C_0 and C_t (mg/L) are influent and effluent concentrations, K_{YN} is the Yoon-Nelson rate constant (min⁻¹), τ is the time when the column reaches 50% adsorbate breakthrough. This model is based on the assumption that the decreasing rate for each adsorbate molecule is proportional to the probability of adsorption and breakthrough on the adsorbent [28].

Parameters obtained using the Yoon-Nelson model for different flow rates and different initial concentrations of NH₄⁺-N, NO₂⁻-N, and NO₃⁻-N are given in Table 3 and Table 4. An increase in flow rate and initial concentration caused an increase in K_{YN} and a decrease in τ . Furthermore, the time when the column reaches 50% breakthrough (τ) as predicted by the Yoon-Nelson model was smaller than the experimental data. This may be caused by the model being linear and thus not being able to fully consider all the adsorption in the columns. Similarly, Karadag et al. studied NH₄⁺ adsorption to clinoptilolite-fixed bed columns using

municipal landfill leachate and found that the Yoon-Nelson model provided a good fit to the actual data [10]. The Yoon-Nelson model was applied to investigate the breakthrough behavior of ammonium at different influent flow rates and influent $\text{NH}_4^+\text{-N}$ concentrations by Simon et al. for the treatment of anaerobically digested swine slurry. The calculated values of K_{YN} and τ showed that an increase in the flow rate and initial $\text{NH}_4^+\text{-N}$ concentration resulted in an increase in the bed sorption rate (K_{YN}) [11].

3.2.3. BDST model

The BDST model is widely used for describing the adsorption process in column experiments for different column heights. The BDST model can be represented by:

$$t = \frac{NZ}{C_0V} - \frac{1}{K C_0} \ln\left(\frac{C_0}{C_t} - 1\right) \quad (3)$$

where C_0 and C_t (mg/L) are influent and effluent concentrations, K (L/mg/h) is the adsorption rate constant, V (cm/h) is the flow rate of the unit surface area through the seepage column, Z (cm) is the column depth, and N (mg/L) is the adsorption capacity. This model is based on the assumption that intraparticle mass transfer resistance and external film resistance can be neglected [29].

As can be observed from Table 5, the fitted linear correlation coefficients using the BDST model were all greater than 0.96, indicating good fitting. For the different seepage column filled heights, the adsorption rates for nitrogen in groundwater were in agreement with the BDST model. The adsorption rate constant K was observed to decrease as the values of C_t/C_0 increased. This indicated that in the seepage column experiments conducted, the adsorption process onto scoria improved and the concentration gradient for the inner and outer adsorbent decreased with time. This led to a decrease in the dynamic transfer force. Consequently, the adsorption rate also decreased. In addition, the rise in C_t/C_0 indicated that the operation of the adsorption columns improved, the residence time was prolonged, and the adsorption amount of unit volume of the adsorption column had an increasing trend. Therefore, the adsorption capacity N became larger at this time.

The results from studies by other researchers are largely in agreement with the findings of the present study. Na et

al. investigated the feasibility of using rice husks as a biosorbent for the removal of ammonium ions from aqueous solutions. They applied the BDST model to experimental data obtained from the fixed bed columns with varying bed heights and found that the model was suitable for simulating the complete breakthrough curve [30]. Simon et al. evaluated ammonium adsorption in biochar-fixed beds for the treatment of anaerobically digested swine slurry. The high correlation values obtained indicated that the BDST model results fitted the experimental data well [11].

3.3. Time and effect of back flush

Regeneration of adsorbent for subsequent reuse can significantly reduce material costs. The back-flush method can enable scoria to recover purification efficiency. In the back-flush experiment, the influent pattern is up-flow, unlike the seepage column reactor experiments. The back-flush flow rate was determined from the rate needed to disturb the scoria and slightly increase its height at the top of the seepage column. This established a flow rate of about 400 mL/min as the back-flush flow rate. In the first 2 min of this experiment, the turbidity of the effluent was high. After 2 min the effluent began to be clear. After a further 2 min the effluent was completely clear. The nitrogen concentration in the effluent was tested for different back-flush times. It was observed that after 15 min, the nitrogen concentration was essentially nil, and thus the back-flush time was determined to be 15 min. The results of seven back flushes are shown in Fig. 6. The regeneration rates were all more than 90%. Therefore, in the purification of nitrogen-contaminated groundwater, scoria can be recycled by using back flushing. This has cost-saving benefits and reduces engineering problems. This is particularly the case in the application of extraction treatment technology where back flushing may prevent blocking, and the equipment can be used for recycling.

Similar conclusions were reached by other researchers using other sorbents. The regeneration ability of functionalized zeolite columns was optimized using 0.1 mol/L Na_2CO_3 solution as a regenerant [25]. Na et al. found that rice husk sorbent could be regenerated by a simple acid washing process without a serious lowering of the sorption capacity or physical durability [30].

Table 5
Parameters estimated by the BDST model for different filled heights

Item	C_t/C_0	N (mg/L)	K (L/mg/h)	R^2
$\text{NH}_4^+\text{-N}$	0.2	108	1.06	0.964
	0.4	216	0.405	0.964
	0.7	240	0.039	0.995
$\text{NO}_2^-\text{-N}$	0.2	108	1.06	0.964
	0.4	180	0.81	0.964
	0.7	228	0.084	0.987
$\text{NO}_3^-\text{-N}$	0.2	1440	0.14	0.979
	0.4	2520	0.0074	0.993
	0.7	2700	0.0053	0.997

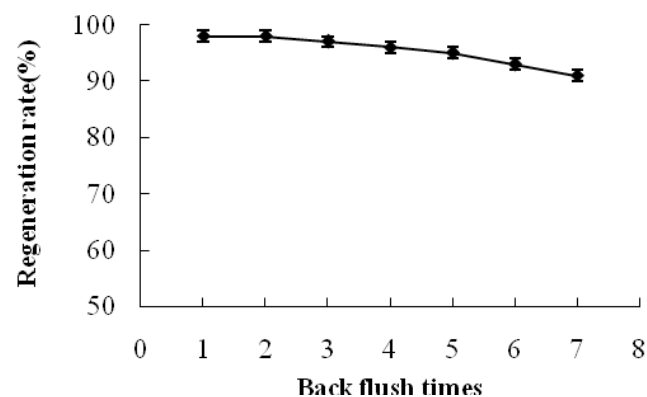


Fig. 6. Back-flush regeneration rate.

3.4. Seepage tank reactor adsorption performance

The flow rate was set at 60 mL/min, and the influent concentration (mg/L) of $\text{NH}_4^+\text{-N}$, $\text{NO}_2^-\text{-N}$, and $\text{NO}_3^-\text{-N}$ was 2, 2, and 30, respectively. The Scoria weight was the same as used in the column experiments. Seepage tank reactor adsorption performance over time is shown in Fig. 7. In tank experiments, the breakthrough curves exhibited a similar pattern to those of the column experiments. However, the curves were smoother and in the primary stage C_t/C_0 was low and the change over time was small. At later times the change began to increase and the rate increased with time. When the tank was near to breakthrough, C_t/C_0 also exhibited little change. The breakthrough times for $\text{NH}_4^+\text{-N}$ and $\text{NO}_2^-\text{-N}$ were almost the same as in the column experiments. However, the breakthrough time of $\text{NO}_3^-\text{-N}$ was slightly shorter than in the column experiments. A plausible explanation for this might be that the tank and column shapes were different, and the contact time was longer in the column experiments. Thus, when the influent concentration of $\text{NO}_3^-\text{-N}$ was 30 mg/L (much higher than the 2 mg/L for $\text{NH}_4^+\text{-N}$ and $\text{NO}_2^-\text{-N}$), the adsorption effectivity was lower in the tank than in the column experiments.

The dynamic column adsorption experiments can be used as preliminary laboratory experiments on extraction treatment technology for nitrogen removal from groundwater. In the study area, groundwater may be extracted and then passed through filtration equipment filled with scoria. Different influent flow rates were tested in the present study. It was found that the flow rate and the filter rate should not be set too high. According to the column experiments, the filter rate should not exceed 8.0 m/h.

The dynamic tank adsorption experiments can provide the basis for in situ remediation technology. Scoria can be used as a permeable reactive barrier material. According to the stratigraphic section, the main aquifer in the study area is an unconfined Quaternary unconsolidated sands aquifer, with part of the stratum containing gravels and underlying Cretaceous mud shale. If in situ remediation technology is applied in the study area, a permeable reactive barrier using scoria can be set up for water from the Quaternary aquifer. The underlying Cretaceous mud shale constitutes an impermeable base to the unconfined aquifer.

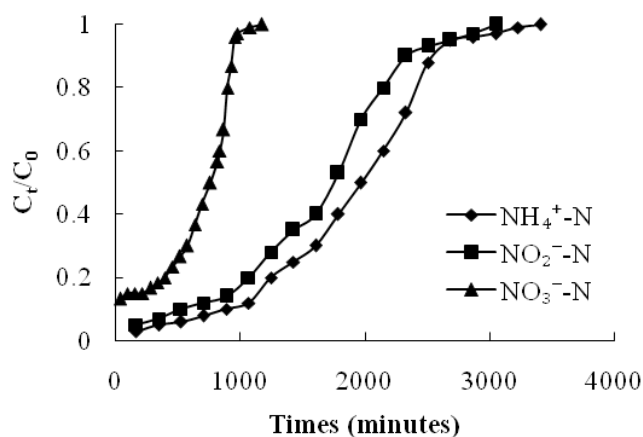


Fig. 7. Seepage tank reactor adsorption performance.

4. Conclusions

Dynamic seepage column and tank experiments were conducted to simulate the purification of nitrogen contaminated groundwater using scoria. These experiments can be used as preliminary experiments determining the extraction treatment technology and permeable reactive barrier technology to be used. The dynamic processes and rules were analyzed and revealed for nitrogen adsorption in aqueous solutions. In column experiments, for high flow rates, high influent concentrations, and low filled heights, the breakthrough point moved to the left and the breakthrough curves became steeper, leading to a lower exhaustion time. At different influent flow rates and different nitrogen concentrations, the adsorption data for nitrogen fitted well with the Thomas and the Yoon-Nelson models. At different material fill heights, the adsorption data fitted well with the BDST model. The back-flush method was shown to improve scoria purification recovery efficiency. After 7 back flushes, the regeneration rate was better than 90%. Tank experiments yielded similar breakthrough curves to column experiments. The breakthrough time of $\text{NH}_4^+\text{-N}$ and $\text{NO}_2^-\text{-N}$ in the tank experiments was almost the same as in the column experiments. However, the breakthrough time of $\text{NO}_3^-\text{-N}$ was slightly shorter than it was in the column experiments.

As an economical, ecologically safe, and practical natural material, scoria can effectively purify groundwater containing nitrogen, and has the capacity to be used in recycling. Scoria can thus be applied in water purification and security engineering.

Acknowledgment

We acknowledge the financial support of the Major Science and Technology Program for Water Pollution Control and Treatment (2014ZX07201010).

References

- [1] F. Faisal, I. Shariff, A.K.M.H. Megat, Adsorption of lead (II) onto organic acid modified rubber leaf powder: Batch and column studies, *Process Saf. Environ. Protection*, 100 (2016) 1–8.
- [2] M.A. Gómez, J. González-López, E. Hontoria-García, Influence of carbon source on nitrate removal of contaminated groundwater in a denitrifying submerged filter, *J. Hazard. Mater.*, 80 (2000) 69–80.
- [3] Y.H. Song, G.L. Qiu, P. Yuan, X.Y. Cui, J.F. Peng, P. Zeng, L. Duan, L.C. Xiang, F. Qian, Nutrients removal and recovery from anaerobically digested swine wastewater by struvite crystallization without chemical additions, *J. Hazard. Mater.*, 190 (2011) 140–149.
- [4] S. Mihaela, D. Anca, T. Carmen, Thermodynamic and kinetic study on ammonium removal from a synthetic water solution using ion exchange resin, *Clean Tech. Environ. Policy*, 16 (2014) 351–359.
- [5] H. Huang, X. Xiao, B. Yan, L. Yang, Ammonium removal from aqueous solutions by using natural Chinese (Chende) zeolite as adsorbent, *J. Hazard. Mater.*, 175 (2010) 247–252.
- [6] S. Kadir, S. Ahmet, A. Mehmet, Removal of ammonium ion from aqueous solution by natural Turkish (Yıldızeli) zeolite for environmental quality, *J. Hazard. Mater.*, 141 (2007) 258–263.
- [7] M. Turan, M.S. Celik, Regenerability of Turkish clinoptilolite for use in ammonia removal from drinking water, *J. Water Supply Res. T.*, 52 (2003) 159–166.

- [8] Y. Yao, B. Gao, M. Zhang, M. Inyang, A.R. Zimmerman, Effect of biochar amendment on sorption and leaching of nitrate, ammonium, and phosphate in a sandy soil, *Chemosphere.*, 89 (2012) 1467–1471.
- [9] P. Jun-Boum, L. Seung-Hak, L. Jae-Won, L. Chae-Young, Lab scale experiments for permeable reactive barriers against contaminated groundwater with ammonium and heavy metals using clinoptilolite, *J. Hazard. Mater.*, 95 (2002) 65–79.
- [10] D. Karadag, E. Akkaya, A. Demir, A. Saral, M. Turan, M. Ozturk, Ammonium removal from municipal landfill leachate by clinoptilolite bed columns: breakthrough modeling and error analysis, *Ind. Eng. Chem. Res.*, 47 (2008) 9552–9557.
- [11] K. Simon, W. Shubiao, M.W. Simon, G. Luchen, D. Renjie, Evaluation of ammonium adsorption in biochar-fixed beds for treatment of anaerobically digested swine slurry: Experimental optimization and modeling, *Sci. Total Environ.*, 563–564 (2016) 1095–1104.
- [12] Z. Feleke, Y. Sakakibara, A bio-electrochemical reactor coupled with adsorber for the removal of nitrate and inhibitory pesticide, *Water Res.*, 36 (2002) 3092–3102.
- [13] A.T. Williams, D.H. Zitomer, B.K. Mayer, Ion exchange-precipitation for nutrient recovery from dilute wastewater, *Environ. Sci. Water Res. Tech.*, 1 (2015) 832–838.
- [14] M. Kei, M. Toshitatsu, H. Yasuo, N. Keiichi, N. Tomoki, Removal of nitrate-nitrogen from drinking water using bamboo powder charcoal, *Bioresource Technol.*, 95 (2004) 255–257.
- [15] Z. Wang, H. Guo, F. Shen, G. Yang, Y. Zhang, Y. Zeng, L. Wang, H. Xiao, S. Deng, Biochar produced from oak sawdust by Lanthanum (La)-involved pyrolysis for adsorption of ammonium (NH_4^+), nitrate (NO_3^-), and phosphate (PO_4^{3-}), *Chemosphere*, 119 (2015) 646–653.
- [16] Y. Wu, Y. Wang, J. Wang, S. Xu, L. Yu, C. Philippe, T. Wintgens, Nitrate removal from water by new polymeric adsorbent modified with amino and quaternary ammonium groups: Batch and column adsorption study, *J. Taiwan Inst. Chem. E.*, 66 (2016) 191–199.
- [17] G.L. Min, H.L. Jun, S.H. Sung, Adsorption characteristics of copper ion by Jeju scoria. *Hwahak Konghak*, 40 (2002) 252–258.
- [18] S.K. Jang, T.Y. Seong, O.K. Soon, Sorption of Zn (II) in aqueous solutions by scoria, *Chemosphere.*, 60 (2015) 1416–1426.
- [19] Y. Zhang, Y.L. Zhang, S.Y. Zhang, F. Song, J.Y. Huang, Y. Zhang, X.D. Bai, Utilization of scoria as PRB reactive media for the removal of petroleum hydrocarbon from groundwater, *J. Adv. Mater. Res.*, 535–537 (2012) 2457–2461.
- [20] S.Y. Zhang, Y. Lu, X.Y. Lin, X.S. Su, Y.L. Zhang, Removal of fluoride from groundwater by adsorption onto La (III)–Al (III) loaded scoria adsorbent, *J. Appl. Surface Sci.*, 303 (2014) 1–5.
- [21] A. Mashal, J. Abu-Dahrieh, A. Ahmed, L. Oyedele, N.M. Haimour, A. Al-Haj-Ali, D. Rooney, Fixed-bed study of ammonia removal from aqueous solutions using natural zeolite, *World J. Sci. Tech. and Sustain. Develop.*, 11 (2014) 144–158.
- [22] Y. Zhu, A dynamic-method study of modified porous zeolite pellet adsorption column removing ammonia-nitrogen from water, *Wuhan University of Technology*, (2005) 59–60 (In Chinese).
- [23] H.G. Thomas, Chromatography: a problem in kinetics, *Ann. N. Y. Acad. Sci.*, 49 (1948) 161–182.
- [24] R. Dolphen, N. Sakkayanwong, P. Thiravetyan, W. Nakbanpote, Adsorption of Reactive Red141 from wastewater onto modified chitin, *J. Hazard. Mater.*, 145 (2007) 250–255.
- [25] H. Wang, H. Gui, W. Yang, D. Li, W. Tan, M. Yang, G.J. Barrow, Ammonia nitrogen removal from aqueous solution using functionalized zeolite columns, *Desal. Water Treat.*, 52 (2014) 753–758.
- [26] L. Xie, S. Ding, L. Dong, R. Ma, Study on influencing factors and kinetics of dynamic adsorption of ammonia nitrogen on walnut shell, *J. Shaanxi Univ. of Sci. Tech.*, 34 (2016) 34–38 (In Chinese).
- [27] Y.H. Yoon, J.H. Nelson, Application of gas adsorption kinetics I. A theoretical model for respirator cartridge service life, *Amer. Ind. Hyg. Assoc. J.*, 45 (1984) 509–516.
- [28] K. Vijayaraghavan, K. Palanivelu, M. Velan, Biosorption of copper (II) and cobalt (II) from aqueous solutions by crab shell particles, *Bioresource Technol.*, 97 (2006) 1411–1419.
- [29] Z. Aksu, S.S. Cagatay, F. Gonen, Continuous fixed bed biosorption of reactive dyes by dried *Rhizopus arrhizus*: determination of column capacity, *J. Hazard. Mater.*, 143 (2007) 362–371.
- [30] C.K. Na, M.K. Song, Removal property of ammonia nitrogen from aqueous solution by rice husk grafted with acrylic acid in batch mode and fixed bed columns, *J. Korea Soc. Waste Manage.*, 31 (2014) 487–497.